MOLECULAR AND CELLULAR BIOLOGY, Aug. 2007, p. 5673–5685 Vol. 27, No. 16
0270-7306/07/$08.00+0 doi:10.1128/MCB.00188-07

XIAP Activity Dictates Apaf-1 Dependency for Caspase 9 Activation▽†

Andrew T. Ho,[1,2] Qin H. Li,[1] Hitoshi Okada,[5,6] Tak W. Mak,[2,5,6] and Eldad Zacksenhaus[1,2,3,4]*

Division of Cell and Molecular Biology, Toronto General Research Institute-University Health Network, 67 College Street, Toronto, Ontario, Canada M5G 2M1,[1] and Departments of Medical Biophysics,[2] Laboratory Medicine and Pathobiology,[3] Medicine,[4] and Immunology,[5] University of Toronto, and The Campbell Family Institute for Breast Cancer Research, Princess Margaret Hospital, 620 University Avenue,[6] Toronto, Ontario, Canada M5G 2C1

Received 31 January 2007/Returned for modification 30 March 2007/Accepted 4 June 2007

The current model for the intrinsic apoptotic pathway holds that mitochondrial activation of caspases in response to cytotoxic drugs requires both Apaf-1-induced dimerization of procaspase 9 and Smac/Diablo-mediated sequestration of inhibitors of apoptosis proteins (IAPs). Here, we showed that either pathway can independently promote caspase 9 activation in response to apoptotic stimuli. In drug-treated *Apaf-1*$^{-/-}$ primary myoblasts, but not fibroblasts, Smac/Diablo accumulates in the cytosol and sequesters X-linked IAP (XIAP), which is expressed at lower levels in myoblasts than in fibroblasts. Consequently, caspase 9 activation proceeds in *Apaf-1*$^{-/-}$ myoblasts; concomitant ablation of *Apaf-1* and *Smac* is required to prevent caspase 9 activation and the onset of apoptosis. Conversely, in stimulated *Apaf-1*$^{-/-}$ fibroblasts, the ratio of XIAP to Smac/Diablo is high compared to that for myoblasts and procaspase 9 is not activated. Suppressing XIAP with exogenous Smac/Diablo or a pharmacological inhibitor can still induce caspase 9 in drug-treated *Apaf-1*-null fibroblasts. Thus, caspase 9 activation in response to intrinsic apoptotic stimuli can be uncoupled from Apaf-1 in vivo by XIAP antagonists.

Programmed cell death by apoptosis is an essential process that affects normal development and homeostasis as well as cancer progression and tumor response to antineoplastic therapies (reviewed in references 11 and 43). Apoptosis involves activation of apical (upstream) caspases, including caspase 8 and caspase 9, which subsequently cleave and activate executioner (downstream) caspases such as caspases 3, 6, and 7, and suppression of inhibitors of apoptosis proteins (IAPs). In the extrinsic pathway, death ligands bind cognate receptors on the cell membrane and induce direct recruitment and activation of caspase 8. In the intrinsic pathway, DNA-damaging agents elicit caspase 9 activation indirectly via proapoptotic members of the Bcl-2 protein family, such as Bax and Bak, that induce mitochondrial outer membrane permeabilization (MOMP) (32).

Upon MOMP, a number of apoptogenic factors, including cytochrome *c*, Smac/Diablo, and apoptosis inducing factor (AIF), are released into the cytosol (6, 21, 24, 46, 48). Interaction of cytochrome *c* with a cytosolic apoptosis protease-activating factor, Apaf-1, induces recruitment of procaspase 9 into a high-molecular-weight complex, termed the apoptosome (52). Aggregation of procaspase 9 at the apoptosome promotes dimerization, which activates the zymogen; dimer-induced autocleavage of caspase 9 further stabilizes its active state (3, 18, 30). A high concentration of purified procaspase 9 induces caspase activation and autocleavage in vitro even in the absence of Apaf-1, though formation of the apoptosome accelerates this process by an order of magnitude (3, 18, 30). The processed, activated caspases are antagonized by direct interaction with the X-linked IAP, XIAP (8, 40, 47). While XIAP is a bona fide inhibitor of caspases, other members of the IAP family, including cIAP-1 and cIAP-2, may not function as caspase inhibitors in vivo but rather prevent apoptosis by other means (7, 8). A second mitochondrial-derived activator of caspases, Smac/Diablo, binds and neutralizes XIAP, allowing executioner caspases to target a plethora of intracellular molecules, ultimately leading to cell demise (reviewed in reference 19).

Inactivation of Bax and Bak or overexpression of the survival factors Bcl-2 and Bcl-x_L inhibits MOMP and confers long-lasting resistance to a variety of intrinsic apoptotic stimuli (25, 32, 49). Persistent apoptotic stimulation and mitochondrial permeabilization are believed to mark a point of no return, after which cells die even in the absence of caspase activation, presumably through AIF or other mechanisms (2, 4, 5, 9, 45). Nonetheless, apoptosis may be delayed and cells may survive transient apoptotic insults that induce MOMP and cytochrome *c* release as long as activation of the caspases fails (10). This is evident from the survival of neurons in *Apaf-1*$^{-/-}$ and *caspase 9*$^{-/-}$ mutant embryos (13, 50), the resistance to apoptosis conferred by a combination of mutations in *caspase 3* and *caspase 7* (22), and the enhanced survival of tumor cells expressing reduced levels of Apaf-1 or high levels of XIAP (39, 41).

Both the cytochrome *c*-Apaf-1 and Smac/Diablo-IAP axes are thought to be required for caspase 9 activation (reviewed in reference 37). Indeed, in *Drosophila melanogaster*, the widespread cell death seen in IAP (*Diap1*) mutant flies is inhibited by loss-of-function mutations in the *Apaf-1* homolog *Dark*, suggesting that apoptosis via the intrinsic pathway is absolutely dependent on Apaf-1 activity (36). Cooperation between these axes for caspase 9 activation is also suggested by the observations cited above that mutations in *Apaf-1* or *caspase 9* in the mouse inhibit apoptosis in certain, but not all, cell types (13, 50) and that down-regulation of Apaf-1 or overexpression of XIAP suppresses apoptosis in human cancer cells (39, 41). However, the effect of each axis alone, cytochrome *c*-Apaf-1 or

* Corresponding author. Mailing address: Division of Cell & Molecular Biology, Toronto General Research Institute-University Health Network, 67 College Street, Rm. 407, Toronto, Ontario, Canada M5G 2M1. Phone: (416) 340-4800, ext. 5106. Fax: (416) 340-3453. E-mail: eldad.zacksenhaus@utoronto.ca.

† Supplemental material for this article may be found at http://mcb.asm.org/.

▽ Published ahead of print on 11 June 2007.

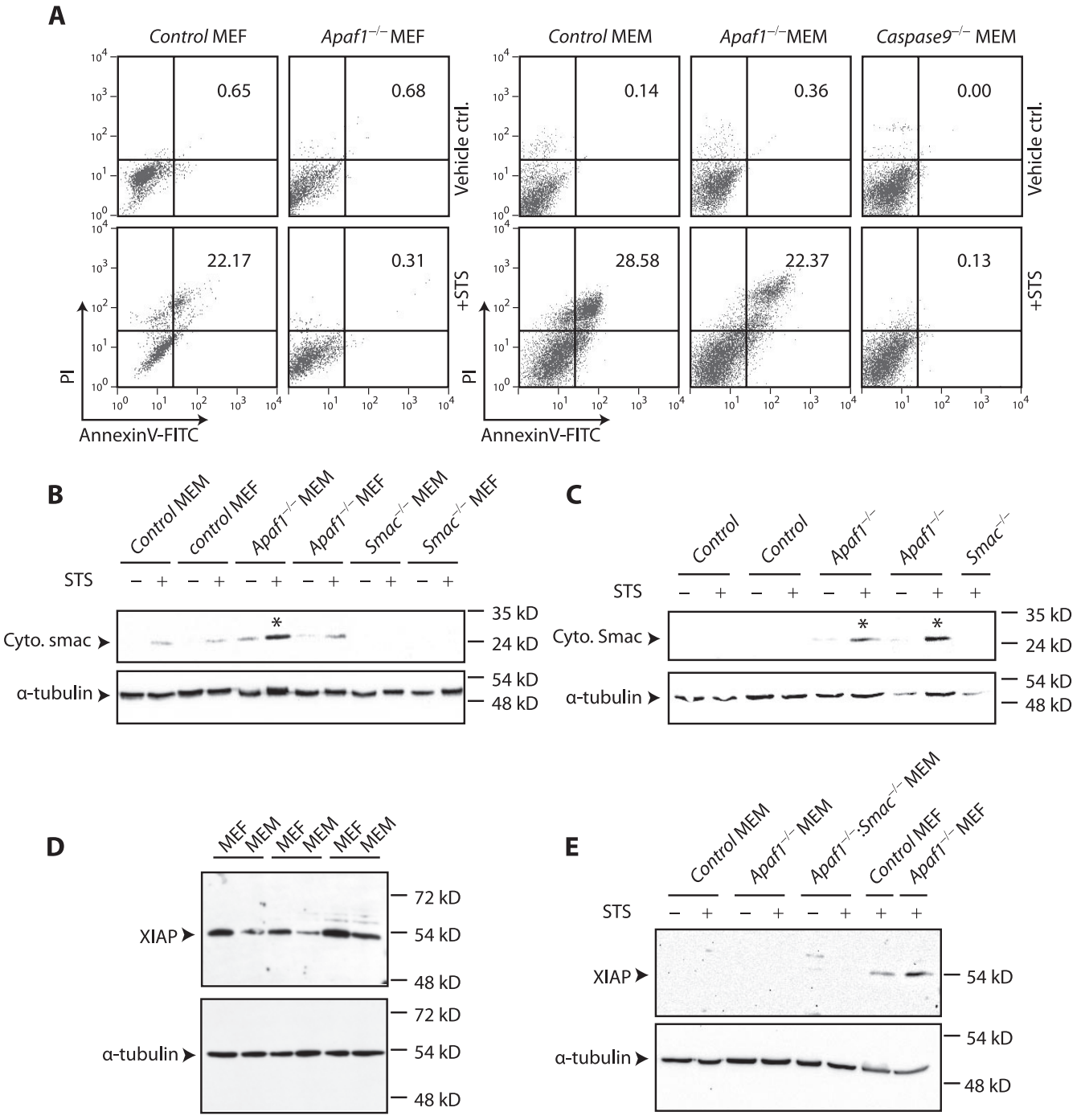

FIG. 1. The caspase 9-dependent, Apaf-1-independent apoptotic response in myoblasts correlates with a high cytosolic Smac/Diablo-to-XIAP ratio. (A) Uncoupling of caspase 9 from Apaf-1. The indicated MEFs or MEMs were exposed to 2 μM STS for 4 h and analyzed by an annexin V binding assay and flow cytometry. Both control cultures were of *Apaf-1*$^{+/-}$ cells. (B) Accumulation of Smac/Diablo in mitochondrion-depleted cytosol fractions from STS-treated *Apaf-1*$^{-/-}$ myoblasts (indicated by asterisks). The control cultures in this and all subsequent panels were of wild-type (e.g., *Apaf-1*$^{+/+}$) cells. (C) Similar analysis as for panel C, with indicated primary myoblasts. (D and E) Two experiments with different exposures demonstrating differential expression of XIAP in myoblasts versus fibroblasts. Western blots of total protein lysates (40 μg) isolated from the indicated cultures were analyzed with antibodies reactive to XIAP. α-Tubulin was used as a loading control. ctrl., control; PI, propidium iodide; FITC, fluorescein isothiocyanate; Cyto., cytosolic.

Smac/Diablo-XIAP, on caspase 9 activation and apoptosis has not been investigated in mammalian cells. Here we showed that in drug-treated primary myoblasts and fibroblasts, caspase 9 activation and caspase 9-mediated apoptosis can be induced independently of Apaf-1, provided that XIAP and/or related proteins are antagonized. Our findings suggest a model in which the cytochrome *c*-Apaf-1 and Smac/Diablo-XIAP axes can independently induce caspase 9 activation in stimulated

cells in vivo and point to the involvement of an additional mitochondrial factor, yet to be unraveled, in this process.

MATERIALS AND METHODS

Mice. *Apaf-1*$^{-/-}$, *Casp9*$^{-/-}$, *Smac*$^{-/-}$, and *Apaf-1*$^{-/-}$ *Smac*$^{-/-}$ embryos were obtained by intercrossing *Apaf-1*$^{+/-}$, *Casp9*$^{+/-}$, *Smac*$^{+/-}$, and *Apaf-1*$^{+/-}$ *Smac*$^{+/-}$ heterozygote mice. The day of vaginal plug observation was considered embryonic day 0.5 (E0.5). PCR-based genotyping was performed on duplicate tissues as previously described (13, 28, 50). Mice were maintained in accordance with the Canadian Animal Care Council.

Isolation and propagation of primary myoblasts and fibroblasts. Limb muscles were removed from E16.5 embryos under a dissecting microscope; isolation and culturing of myoblasts were performed as previously described (15). Primary fibroblasts were isolated from the skin of the same embryos. Primary cultures were used by the fourth passage.

Long-term cell survival by MTT assay. Briefly, 3,000 cells/well were seeded in 24-well plates and grown overnight. After a 4-h drug treatment, the cells were washed with PBS and cultured in normal media for an additional 72 h. An MTT [3-(4,5-dimethylthiazol-2-yl)-(2,5-diphenyl-tetrazolium bromide] assay was performed as previously described (15).

Immunofluorescent and confocal microscopy. Subconfluent cell cultures, grown on collagen 1-coated glass coverslips (Biocoat/VWR), were fixed in 4% paraformaldehyde in phosphate-buffered saline (PBS) at room temperature for 5 min. For multiple immunofluorescent labeling, the coverslips were treated with extraction buffer (1 mM EGTA, 4% polyethylene glycol 8000, 0.1 M 1,4-piperazine-bis-ethanesulfonic acid [pH 6.9], and 0.1% Triton X-100) for 5 min, followed by three washings in PBS and 5 min of blocking with 1% bovine serum albumin-PBS. The coverslips were incubated with anti-α-tubulin antibody (1:100 dilution; Sigma-Aldrich, MI) and anti-MyoD (1:50 dilution; Santa Cruz, CA) in blocking solution for 45 min in a humidified chamber at room temperature. After being washed three times for 5 min each in PBS, the samples were incubated for 45 min with 1:200 dilutions of Alexa 568 (red) and Alexa 488 (green) secondary antibodies (Molecular Probes). For Smac/Diablo labeling, cells were grown on collagen 1 coverslips, incubated with 300 nM MitoTracker Red 580 (Molecular Probes) for 30 min, fixed in 100% methanol (prechilled at −20°C) for 5 min, and placed in blocking solution (1% bovine serum albumin/PBS). Anti-Smac/Diablo antibody (1:100 dilution; Alexis) in blocking solution was added for 45 min at room temperature. After being washed three times in PBS, the coverslips were incubated with Alexa 488 (Molecular Probes) goat anti-rabbit secondary antibody at a dilution of 1:100 and 10 μg/ml Hoechst (Sigma) in blocking solution. Specimens were mounted with fluorescent media (Dakocytomation) and sealed with nail enamel. Confocal images of 0.5-μm optical sections were captured, using a ×63 c-apochromat objective lens on an LSM 510 Zeiss Axiovert 100 M confocal microscope.

Annexin V and TUNEL assays for cell culture. Subconfluent cultures were trypsinized to obtain single-cell suspensions, washed once in binding buffer (10 mM HEPES, 140 mM NaCl, 5 mM KCl, 1 mM $MgCl_2$, and 1.8 mM $CaCl_2$ [pH 7.4]) and stained with propidium iodide (10 μg/ml) and annexin V-fluorescein isothiocyanate (25 μg/ml). For experiments with green fluorescent protein (GFP), annexin V-phycoerythrin (PE) (25 μg/ml) was used. After 20 min at room temperature, the cells were washed once with binding buffer and quantified, using a FACSCalibur flow cytometer (BD Biosciences, San Jose, CA). Ten thousand events were counted for each sample. Cells undergoing DNA fragmentation were detected by flow cytometry, using a modified terminal deoxynucleotidyltransferase-mediated dUTP-biotin nick end labeling (TUNEL) protocol. Briefly, 2×10^6 staurosporine (STS)-treated and control cells were fixed in 4% paraformaldehyde, digested for 1 min digestion in 0.1% trypsin, and washed twice in PBS. The cells were labeled with 10 μM fluorescein-dUTP (Boeringer Manheim) by terminal deoxynucleotidyl transferase (100 U/ml; Boeringer Manheim) at 37°C for at least 1 h and washed twice with PBS prior to being analyzed by flow cytometry.

Western blotting. Apoptosis was induced by adding 2 μM STS for the duration specified in each experiment. Cells were lysed in CHAPS {3-[(3-cholamidopropyl)-dimethylammonio]-1-propanesulfonate} cell extraction buffer {50 mM PIPES [piperazine-*N*,*N*′-bis(2-ethanesulfonic acid)]/HCl [pH 6.5], 2 mM EDTA, 0.1% CHAPS [Sigma], 20 μg/ml leupeptin, 10 μg/ml pepstatin A, 10 μg/ml aprotinin, 5 mM dithiothreitol [DTT], and 1 mM phenylmethylsulfonyl fluoride}. Cytosolic and mitochondrial fractions were isolated by a modified subcellular fractionation protocol provided with the mitochondrial fractionation kit (Active Motif). Briefly, cell pellets were resuspended in a hypotonic buffer (10 mM HEPES [pH 7.9], 10 mM KCl, 0.1 mM EDTA, 0.1 mM EGTA, 1 mM DTT, 0.5 mM phenylmethylsulfonyl fluoride, and 1% [vol/vol] aprotinin) for 30 min on ice and lysed either by Dounce homogenization or by flash freezing and thawing three times. Sequential centrifugation was used to isolate the mitochondrial and cytosolic fractions. First centrifugation at 800 × *g* for 20 min was used to remove unlysed nuclei and insoluble cell debris. The supernatant was then subjected to 10,000 × *g* for 30 min to separate the mitochondrial fraction (pellet) from the cytosolic fraction (supernatant). Forty micrograms of each sample was separated by 10% sodium dodecyl sulfate-polyacrylamide gel electrophoresis, Western blotted onto nitrocellulose membranes, and immunodetected, using mouse-specific caspase 9 polyclonal antibodies (Cell Signaling) at a dilution of 1:1,000 in 2.5% skim milk-TBST (Tris-buffered saline containing 10 mM Tris-HCl [pH 8.0], 150 mM NaCl, and 0.05% Tween 20) or anti-activated caspase 9 antibody at a dilution of 1:200 (Santa Cruz Biotechnology) and anti-rabbit immunoglobulin G-horseradish peroxidase (HRP)-conjugated secondary antibody at a dilution of 1:2,000 in 2.5% skim milk-TBST (Cell Signaling). Antibodies for Smac and XIAP (ProSci Inc.), poly(ADP-ribose) polymerase (PARP; Cell Signaling), cIAP1 (R & D Systems, Inc.), and cytochrome *c* (clone A-8; Santa Cruz Biotech) were used at dilutions of 1:1,000 in 5% skim milk-TBST and incubated with the appropriate HRP-conjugated secondary antibody (Cell Signaling) at dilutions of 1:2,000 in 5% skim milk-TBST. Incubation with goat anti-fast skeletal troponin T (1:100 dilution; Santa Cruz Biotech) in 5% milk-TBST was followed by incubation with secondary donkey anti-goat HRP antibody (at a 1:2,000 dilution in 5% skim milk-TBST; Santa Cruz Biotech). Anti-α-tubulin antibody (1:1,500 dilution in 5% skim milk-TBST; Sigma) was used with anti-mouse immunoglobulin G-HRP antibody (1:3,000 dilution in 5% milk-TBST; Cell Signaling). HRP activity was visualized by using SuperSignal West Dura chemiluminescence substrate (Pierce) and was captured digitally by a Bio-Rad Flour-S-Max multimager equipped with a Nikon CCD camera or by using X-ray films.

In vitro caspase activity assays. In vitro caspase activities were performed according to the instructions for the ApoAlert caspase kit (Clontech/BD Biosciences). Briefly, after being exposed to apoptotic stimuli, cell pellets were lysed with an equal volume of 2× DTT reaction mix provided by the manufacturer. After a 30-min incubation on ice, 250 μM of caspase 9 substrate (LEHD-aminomethyl coumarin) or caspase 3 substrate (DEVD-aminomethyl coumarin) was added to each sample (10 μg). The reaction was carried out in buffer containing 100 mM HEPES [pH 7.5], 20% glycerol, 5 mM DTT, and 0.5 mM EDTA [pH 8.0] at 37°C for 1 h. Caspase 9 and caspase 3 activities were measured by a GENios fluorometer (Tecan) at wavelengths of 400 nm excitation/505 nm emission and 380 nm excitation/460 nm emission, respectively.

Histology and TUNEL analysis on sections. Briefly, embryos were fixed in 4% paraformaldehyde at 4°C overnight, dehydrated, and embedded in paraffin. Sections 8 μm thick were stained with hematoxylin and eosin, and TUNEL assays were performed using biotin-dUTP followed by 3,3′diaminobenzidine tetrahydrochloride staining (51).

pSmac$^{\Delta MTS}$-IRES2-eGFP construction and transfection. PCR was used to amplify a DNA fragment containing amino acids 54 to 237 of Smac. The 5′ primer (5′-ATACTCGAGCCACCATGGCGGTTCCTATTGCTCAG-3′) included an XhoI site, an optimal Kozak CGACCATG sequence with a methionine fused to A54 in the mouse Smac gene, thereby deleting the first 53 amino acids of the protein that contains the mitochondrial targeting sequence (MTS). The 3′ primer (5′-TAAGGATCCTCAATCTTCACGCAGGTAGGC-3′) contained a stop codon followed by a BamH1 site. The PCR product was purified, digested with Xho1 plus BamH1, and subcloned into pIRES2-eGFP (Clonetech/BD Bioscience). Sequence analysis confirmed the in-frame deletion and lack of unwanted, inadvertent mutations. Transfection of primary cells with pSMAC$^{\Delta MTS}$-IRES2-eGFP was performed using a Lipofectamine 2000 kit (Invitrogen). Briefly, subconfluent cells were incubated with a 1:3 ratio of DNA (μg) to Lipofectamin (μl) in serum-free Opti-MEM I medium (Invitrogen) for 8 h at 37°C. The medium was replaced with 10% fetal bovine serum-Dulbecco's modified Eagle's medium, and cultures were analyzed 24 h later.

TABLE 1. Frequency of live progeny from *Apaf-1* and *Smac* heterozygous intercrosses at E16.5

Genotype	No. (%) of live embryos expected	No. (%) of live embryos observed
Control[a]	168 (56.25)	172 (57.72)
Apaf-1$^{-/-}$[b]	56 (18.75)	49 (16.44)
Smac$^{-/-}$	56 (18.75)	61 (20.47)
Apaf-1$^{-/-}$ *Smac*$^{-/-}$[c]	18 (6.25)	16 (5.37)

[a] Includes *Apaf-1*$^{+/\pm}$ and/or *Smac*$^{+/\pm}$ genotypes.
[b] Eight of 49 (16.32%) embryos had protruded brain morphology.
[c] Three of 16 (18.75%) embryos had protruded brain morphology.

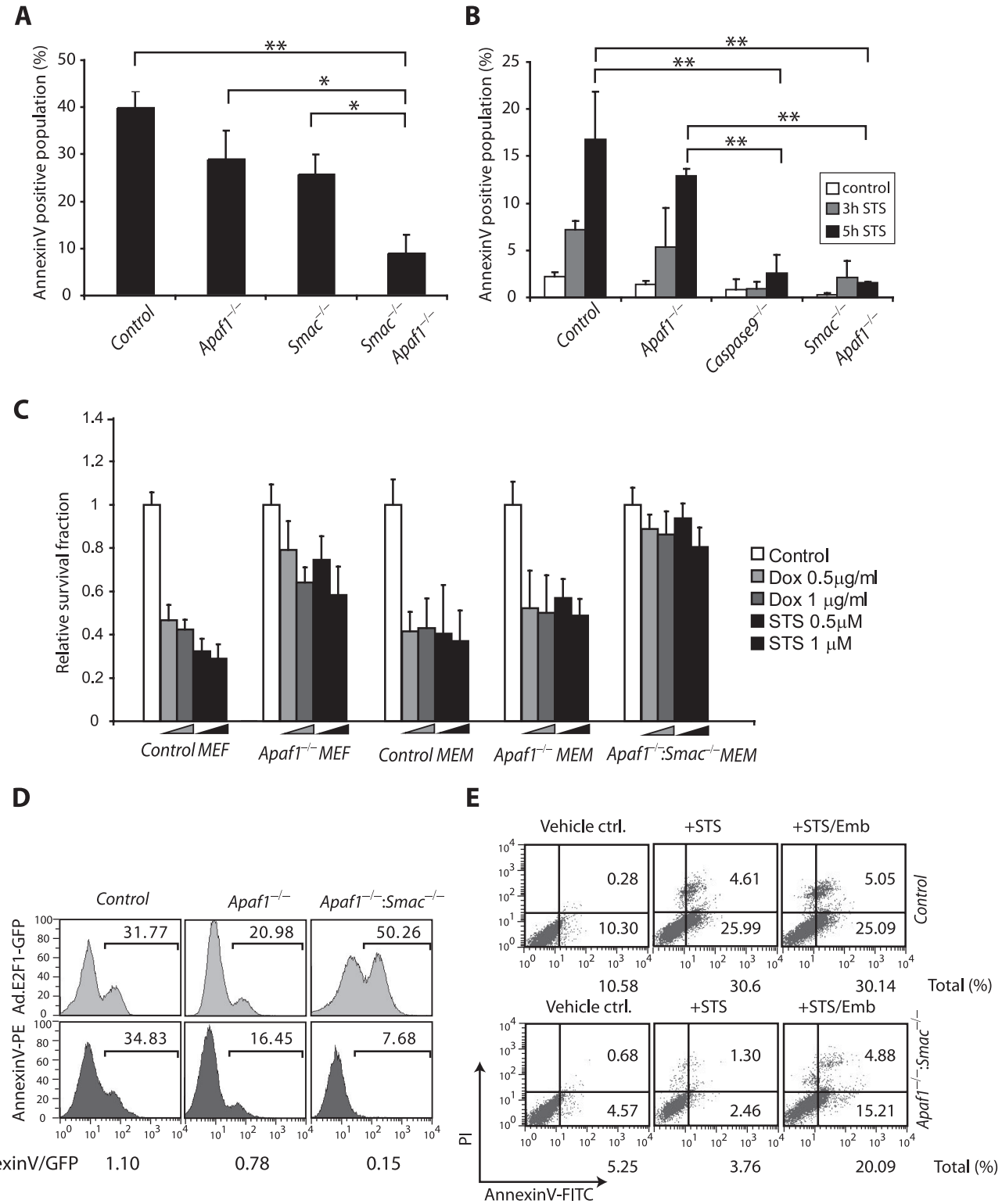

FIG. 2. Combined loss-of-function mutations in *Apaf-1* and *Smac* confer resistance to transient exposure to apoptotic stimuli in primary myoblast cultures: reversal by embelin. (A) The indicated littermate cultures were treated with STS for 5 h, and early apoptosis was assessed by a fluorescein isothiocyanate-annexin V binding assay followed by flow cytometry analysis. Each bar graph and error bar represents the average and standard deviation calculated from three independent experiments. * and ** denote a significant difference at $P < 0.05$ and $P < 0.001$, respectively, as determined by the Student *t* test. (B) Similar experiment as for panel A, comparing the apoptosis levels of *Apaf-1*$^{-/-}$ *Smac*$^{-/-}$ MEMs to those of the control, *Apaf-1*$^{-/-}$, and *caspase 9*$^{-/-}$ MEMs 0, 3, and 5 h posttreatment. (C) Similar long-term survival rates of *Apaf-1*$^{-/-}$ *Smac*$^{-/-}$ MEMs and *Apaf-1*$^{-/-}$ MEFs following transient exposure to apoptotic stimuli. Cultures were treated for 4 h with the indicated concentrations of STS or doxorubicin, washed, and replated in 6 wells per culture in 24-well plates. Three days later, cell proliferation/survival was assessed by an MTT assay.

RESULTS

Uncoupling of caspase 9 activation from Apaf-1 in stimulated primary myoblasts correlates with accumulation of cytosolic Smac/Diablo. Previously, we showed that in contrast to fibroblasts, where Apaf-1 is required to process procaspase 9, skeletal myoblasts undergo Apaf-1-independent caspase 9 activation and apoptosis (12, 15). This is demonstrated in Fig. 1A, for which we used a fluorescent-based annexin V binding assay, which detects phosphatidylserine residues that translocate to the outer cell membrane during early stages of apoptosis. Exposure of primary embryonic fibroblasts (MEFs) to 2 μM STS for 4 h induced annexin V reactivity in 22% of the cells, whereas *Apaf-1*$^{-/-}$ (and *casp9*$^{-/-}$; data not shown) fibroblasts were highly resistant (0.3%) (Fig. 1A, left panels). In contrast, embryonic myoblasts (MEMs) exhibited early signs of apoptosis in the absence of *Apaf-1* (22%) but not in the absence of *caspase 9* (0.1%) (Fig. 1A, right panels). Thus, in mammals, the coupling of caspase 9 activation to Apaf-1 is cell type specific.

After various considerations (16) and numerous trials to define the mechanism of Apaf1-independent apoptosis, we explored the expression of IAPs and Smac/Diablo in these two cell lineages. To test the levels of Smac, mitochondrion-free cytosols from STS-treated or untreated cells were isolated, using hypotonic lysis conditions and differential centrifugations. Remarkably, the levels of Smac/Diablo were reproducibly higher in the cytosolic fractions from STS-treated *Apaf-1*$^{-/-}$ myoblasts than in the control myoblasts, fibroblasts, or *Apaf-1*-deficient fibroblasts (Fig. 1B and C show two independent experiments with different exposures). Low levels of cytosolic Smac/Diablo were observed in *Apaf-1*$^{-/-}$ myoblasts even under nonstimulating conditions and significantly increased upon STS treatment. A similar increase in Smac/Diablo in STS-treated *Apaf-1*$^{-/-}$ myoblasts was also observed when mitochondrion-free cytosolic fractions were prepared by a freeze-thaw procedure (data not shown). Notably, the kinetics of cytochrome *c* release are similar in the different myoblast and fibroblast cell types (15) (see Fig. 4B), indicating that accumulation of Smac/Diablo in the cytosols of apoptosing *Apaf-1*$^{-/-}$ myoblasts is not due to an indirect effect of Apaf-1 deficiency on mitochondrial integrity. In addition, the total amount of Smac/Diablo was not elevated in drug-treated versus untreated cells, as evident from Western blot analysis of whole-cell lysates and confocal microscopy (see Fig. S1B and C in the supplemental material), indicating that Smac/Diablo accumulated specifically in the cytosols of *Apaf-1*$^{-/-}$ myoblasts following STS treatment. Interestingly, expression of XIAP was reproducibly reduced by at least 50% in myoblasts compared with fibroblasts in both wild-type and *Apaf-1* mutant cells (Fig. 1D and E). Expression of another IAP member, cIAP-1, was also lower in myoblasts than in fibroblasts (Fig. S1A). Thus, upon apoptotic stimulus, the cytosolic Smac/Diablo-to-XIAP ratio is significantly higher in primary *Apaf-1*$^{-/-}$ myoblasts than in primary *Apaf-1*$^{-/-}$ fibroblasts.

***Apaf-1*$^{-/-}$ *Smac*$^{-/-}$ double mutant myoblasts resist early onset of apoptosis.** The aforementioned results suggest that the susceptibility of *Apaf-1*$^{-/-}$ myoblasts to apoptotic stimuli may be due to efficient sequestration of XIAP by Smac/Diablo in these cells. If this notion is correct, inactivation of both *Apaf-1* and *Smac* should increase the effective level of XIAP and inhibit caspase 9 activation and apoptosis. To test this idea, we interbred *Apaf-1*$^{+/-}$ and *Smac*$^{+/-}$ knockout mice to generate double mutant embryos. Most *Apaf-1*$^{-/-}$ embryos on a 129/sv × C57BL/6 mixed background die in utero with craniofacial abnormalities and reduced apoptosis in the brain (50). In contrast, *Smac*$^{-/-}$ mutant mice are viable and sensitive to both intrinsic and extrinsic apoptotic stimuli (28). *Apaf-1*$^{-/-}$ *Smac*$^{-/-}$ double mutant embryos were recovered at embryonic day E16.5 with near-Mendelian inheritance (Table 1). Histology and apoptosis assays failed to detect obvious differences between *Apaf-1*$^{-/-}$ *Smac*$^{-/-}$ and *Apaf-1*$^{-/-}$ embryos (see Fig. S2 in the supplemental material). Primary myoblasts were isolated from the soleus muscles of *Apaf-1*$^{-/-}$ *Smac*$^{-/-}$ and control embryos, expanded, and used by passage 2 to 4 to avoid senescence. A total of over 16 independent primary *Apaf-1*$^{-/-}$ *Smac*$^{-/-}$ and over 40 *Apaf-1*$^{-/-}$ mutant cultures were generated for this study, and at least three independent primary cultures were analyzed per experiment.

After exposure to apoptotic stimuli, *Apaf-1*$^{-/-}$ and *Smac*$^{-/-}$ myoblasts underwent a robust apoptotic response which was approximately 75% of the level observed in wild-type cells, as measured by an annexin V binding assay, (Fig. 2A). Strikingly, *Apaf-1*$^{-/-}$ *Smac*$^{-/-}$ double mutant myoblasts exhibited only background levels of annexin V binding under the same conditions. We extended this analysis to compare the *Apaf-1*$^{-/-}$ *Smac*$^{-/-}$ double mutant myoblasts with *caspase 9*$^{-/-}$ myoblasts, which are highly resistant to intrinsic apoptotic signals (15) (Fig. 1A, right panel). Remarkably, time course experiments demonstrated that the *Apaf-1*$^{-/-}$ *Smac*$^{-/-}$ myoblasts were as resistant to STS treatment as the *caspase 9*$^{-/-}$ myoblasts (Fig. 2B).

To test whether the *Apaf-1*$^{-/-}$ *Smac*$^{-/-}$ mutations conferred long-term survival, the various cell types were treated with lower doses of STS (0.5 and 1 μM) for 4 h. The cells were then washed to remove the drug and cultured for 3 days in drug-free media. At this stage, the number of cells was evaluated by measuring mitochondrial reductase activity by a colorimetric MTT assay. As shown in Fig. 2C, the *Apaf-1*$^{-/-}$ *Smac*$^{-/-}$ myoblasts exhibited a twofold increase in resistance to transient exposure to STS relative to the control myoblasts. Importantly, the level of resistance to STS exhibited by the *Apaf-1*$^{-/-}$ *Smac*$^{-/-}$ myoblasts was similar to that of the *Apaf-1*$^{-/-}$ fibroblasts. Comparable results were also obtained with the clinically relevant cytotoxic drug doxorubicin (Adriamycin) (Fig. 2C).

To further test the resistance of *Apaf-1*$^{-/-}$ *Smac*$^{-/-}$ myoblasts to apoptotic stimuli, we infected the various primary cultures with a recombinant adenovirus (Ad) vector encoding

(D) Resistance to E2F1-induced apoptosis in *Apaf-1*$^{-/-}$ *Smac*$^{-/-}$ myoblasts relative to that in *Apaf-1*$^{-/-}$ myoblasts. The indicated cultures were infected with an Ad vector encoding E2F1 and GFP and stained 24 h later with phycoerythrin R-annexin V (AnnexinV-PE). Relative apoptosis (annexin V-positive cells) normalized for infection efficiency (GFP-positive cells) is indicated by the AnnexinV/GFP ratio. (E) Restimulation of apoptotic response in *Apaf-1*$^{-/-}$ *Smac*$^{-/-}$ double mutant myoblasts by embelin (Emb). Control (ctrl.) and *Apaf-1*$^{-/-}$ *Smac*$^{-/-}$ myoblast cultures were treated with vehicle (dimethyl sulfoxide), STS (2 μM), or STS plus embelin (30 μM) for 3 h. The total percentage of annexin V-positive cells is indicated below each panel.

E2F1 and GFP; infection efficiency and cell death were quantified by analyzing the GFP- and PE-conjugated annexin V fluorescent signals by flow cytometry. At 16 h post-Ad.E2F1-GFP infection, both the control and *Apaf-1*$^{-/-}$ myoblasts died by apoptosis (~100% and 78%, respectively) (Fig. 2D). In contrast, the double mutant *Apaf-1*$^{-/-}$ *Smac*$^{-/-}$ myoblasts were highly resistant to E2F1-induced apoptosis (15%).

It was important to demonstrate that the resistance of *Apaf-1*$^{-/-}$ *Smac*$^{-/-}$ myoblasts to apoptotic stimuli was not due to contaminating fibroblasts, where loss of *Apaf-1* alone confers cytoprotection. We first ruled out this possibility by analyzing the expression of myogenic markers in the various cultures. Western blot analysis revealed similar levels of expression of troponin T in control, *Apaf-1*$^{-/-}$, and *Apaf-1*$^{-/-}$ *Smac*$^{-/-}$ myoblasts (Fig. 3A). Immunostaining for MyoD also demonstrated similar abundances of MyoD-positive cells in the various myoblast cultures tested (Fig. 3B). Second, we simultaneously labeled MyoD-expressing and apoptosing cells, using a fluorescent TUNEL assay, which marks nuclei with nicked/fragmented DNA, the hallmark of apoptosis. In a representative experiment shown in Fig. 3C, MyoD-positive *Apaf-1*$^{-/-}$ and *Smac*$^{-/-}$ myoblasts exhibited 34% and 37.6% TUNEL-positive cells, respectively, compared with 41% in the control wild-type cells. In contrast, MyoD-positive *Apaf-1*$^{-/-}$ *Smac*$^{-/-}$ double mutant myoblasts analyzed in parallel displayed only 7.1% apoptosis. Thus, combined inactivation of Apaf-1 and Smac/Diablo inhibits early onset of apoptosis specifically in primary skeletal myoblast cells.

Caspase 9 activation is inhibited in *Apaf-1*$^{-/-}$ *Smac*$^{-/-}$ double mutant myoblasts. We next asked whether the early signs of cytoprotection observed in stimulated *Apaf-1*$^{-/-}$ *Smac*$^{-/-}$ mutant myoblasts was accompanied by lack of caspase activation. We first tested the enzymatic activity of caspase 9 using a synthetic substrate, LEHD-AMC, which fluoresces upon cleavage by caspase 9 as well as other caspases (caspases 2 and 10). This assay revealed a significant reduction in LEHD-AMC cleavage in cytosolic extracts from *Apaf-1*$^{-/-}$ *Smac*$^{-/-}$ double mutant myoblasts and *Apaf-1*$^{-/-}$ MEFs compared with those from control wild-type MEMs (Fig. 4A).

To determine whether the reduced enzymatic activity of caspase 9 in *Apaf-1*$^{-/-}$ *Smac*$^{-/-}$ myoblasts was associated with reduced processing of the caspase, we performed Western blots with a murine-specific caspase 9 antibody that recognizes the 49-kDa zymogen as well as the 39- and 37-kDa cleaved forms of the enzyme (23). Processing of procaspase 9 was observed at 4 h in control myoblasts, and it had increased further at 6 h post-STS treatment (Fig. 4B). Caspase 9 cleavage in *Apaf-1*$^{-/-}$ and *Smac*$^{-/-}$ myoblasts followed a similar, albeit slightly delayed, kinetic. In contrast, processing of procaspase 9 was strongly suppressed in *Apaf-1*$^{-/-}$ *Smac*$^{-/-}$ double mutant myoblasts even 6 h post-STS treatment, despite efficient release of cytochrome *c* into the cytosol (Fig. 4B). Densitometry analysis revealed that whereas caspase 9 cleavage increased 12.2-, 12.2-, and 8-fold in the control, *Apaf-1*$^{-/-}$, and *Smac*$^{-/-}$ myoblasts, respectively, it increased by only 1.8-fold in the *Apaf-1*$^{-/-}$ *Smac*$^{-/-}$ compound mutant myoblasts. Inhibition of caspase 9 cleavage in *Apaf-1*$^{-/-}$ *Smac*$^{-/-}$ mutant myoblasts was also observed by using an antibody that reacts exclusively with the processed form of caspase 9 (data not shown).

To further assess the extent of resistance to apoptosis in *Apaf-1*$^{-/-}$ *Smac*$^{-/-}$ myoblasts, we followed caspase 9 processing in these cells over an extended period of time. Cleaved caspase 9 was readily detected in wild-type control, *Apaf-1*$^{-/-}$, and *Smac*$^{-/-}$ myoblasts at 8 and 24 h following exposure to STS (Fig. 4C). In contrast, caspase 9 processing was clearly observed in *Apaf-1*$^{-/-}$ *Smac*$^{-/-}$ myoblasts and *Apaf-1*$^{-/-}$ fibroblasts only 24 h post-STS treatment. Thus, the inhibition of caspase 9 processing conferred by inactivation of both *Apaf-1* and *Smac* in myoblasts was similar to that observed by loss of *Apaf-1* alone in fibroblasts. The eventual activation of caspase 9 may account in part for the cell death observed in *Apaf-1*$^{-/-}$ *Smac*$^{-/-}$ myoblasts and *Apaf-1*$^{-/-}$ fibroblasts after long-term exposure to cytotoxic drugs (Fig. 2C).

Cytosolic lysates prepared from *Apaf-1*$^{-/-}$ *Smac*$^{-/-}$ double mutant myoblasts exhibited a marked reduction in caspase 3/caspase 7 enzymatic activity (with DEVD-AMC substrate) compared with that from control wild-type, *Apaf-1*$^{-/-}$, or *Smac*$^{-/-}$ myoblasts, which was similar to the activity observed in lysates from *caspase 9*$^{-/-}$ mutant myoblasts (Fig. 4D). Cleavage of PARP, a substrate for caspase 3, was readily detected in control wild-type myoblasts within 4 h, and it peaked at 6 h (Fig. 4E). In *Apaf-1*$^{-/-}$ mutant myoblasts, PARP was cleaved in a similar, yet slightly delayed, kinetic. In contrast, PARP cleavage was severely inhibited in *Apaf-1*$^{-/-}$ *Smac*$^{-/-}$ double mutant myoblasts, being undetectable even 8 h post-STS treatment. We concluded that in primary myoblasts, the combined loss of Apaf-1 and Smac/Diablo, but not Apaf-1 alone, inhibits caspase 9 activation and the onset of apoptosis.

A testable model for the role of XIAP in Apaf-1-independent caspase 9 activation. Based on the observations described above, we propose that in drug-treated mammalian cells, procaspase 9 autodimerization and activation are sufficiently robust to occur in the absence of Apaf-1 as long as XIAP or related proteins are kept in check. In *Apaf-1*$^{-/-}$ myoblasts, XIAP is expressed at a relatively low level and further antagonized by Smac/Diablo, which accumulates in the cytosols in these cells in response to MOMP (Fig. 1B to E). In these mutant cells, caspase 9 is activated in the absence of Apaf-1; inactivation of both *Apaf-1* and *Smac* is required to prevent cell death (Fig. 2 to 4 and 5A). In contrast, XIAP is expressed at high levels in fibroblasts, and Smac/Diablo does not accumulate in the cytosol. We hypothesized that in MEFs, loss of *Apaf-1* alone blocks apoptosis because the abundant XIAP traps caspase 9 in an inactive state (40) (Fig. 5B). If this model is correct, inhibition of XIAP should induce caspase 9 activation and apoptotic response in stimulated *Apaf-1*$^{-/-}$ MEFs.

XIAP antagonists induce caspase 9 activation and apoptotic response in *Apaf-1*$^{-/-}$ fibroblasts and *Apaf-1*$^{-/-}$ *Smac*$^{-/-}$ myoblasts. To test this model (Fig. 5B), we inhibited XIAP in *Apaf-1*$^{-/-}$ MEFs by overexpressing Smac/Diablo or by treatment with a pharmacological inhibitor. We constructed a multicistronic plasmid, pSmac$^{\Delta MTS}$-IRES2-eGFP, which encodes a cytosolic Smac$^{\Delta MTS}$ allele with an in-frame deletion of the MTS, as well as GFP. Transfected cells were gated on the basis of GFP expression, and the percentage of PE-annexin V-positive cells within this gated population was determined. When *Apaf-1*$^{-/-}$ MEFs were transfected with an empty vector, pGFP, they retained their characteristic resistance to STS (3.3%) (Fig. 6A, right panels). Remarkably, when transfected

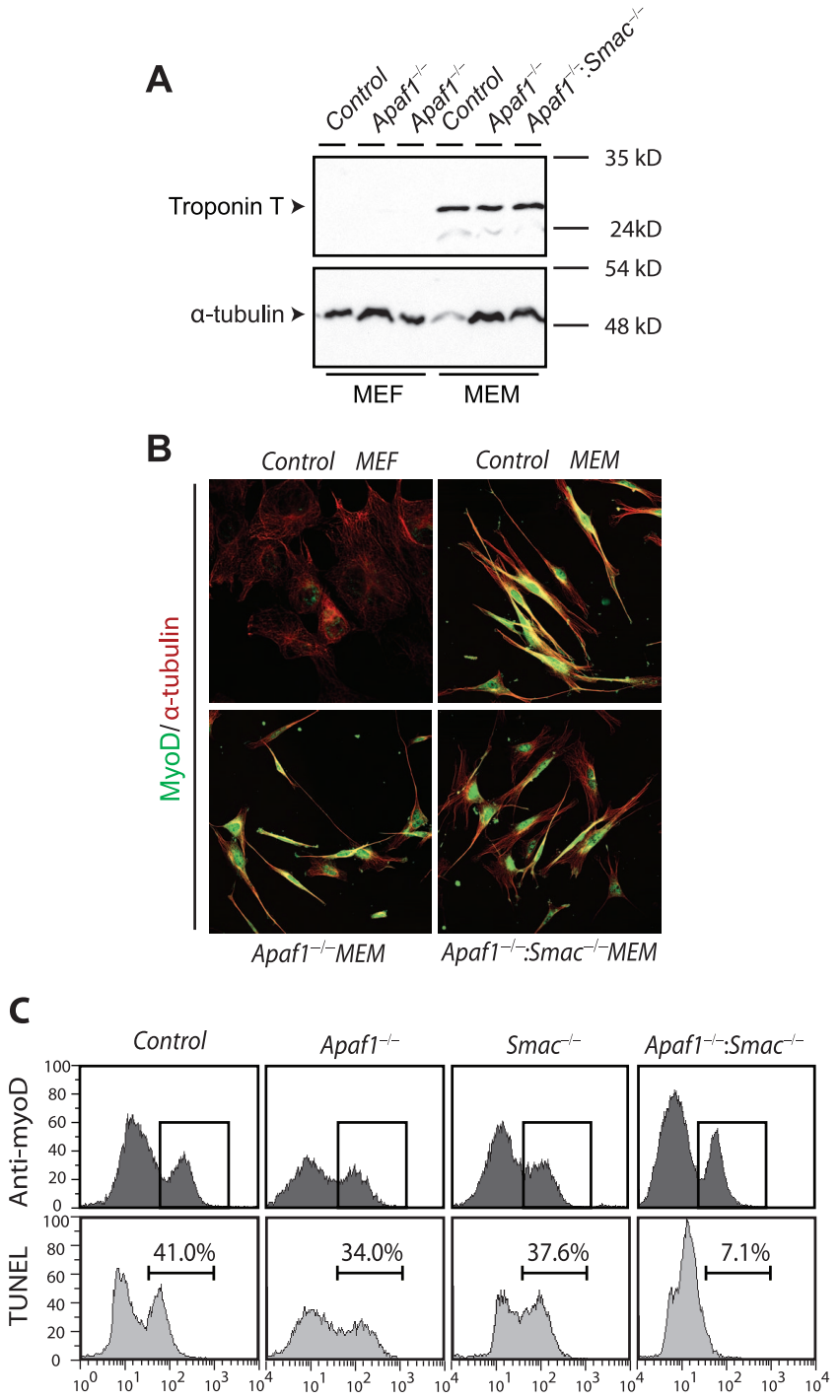

FIG. 3. Combined loss-of-function mutations in *Apaf-1* and *Smac* confer resistance to apoptotic stimuli specifically in the myoblast lineage. (A) Western blot analysis of indicated primary cultures with the myogenic marker troponin T. (B) Immunostaining of the indicated primary cultures with anti-MyoD (green), anti-α-tubulin (red), and DAPI (4′,6′-diamidino-2-phenylindole; blue). (C) The indicated cultures treated with STS for 4 h were double labeled with anti-MyoD and Alexa 568 secondary antibodies to tag MyoD-expressing myoblasts and subjected to fluorescein-dUTP TUNEL to detect apoptotic cells. MyoD-positive cells were first gated (upper rows), and the percentage of TUNEL-positive cells within the gated population was quantified by flow cytometry (lower rows).

with pSmac$^{\Delta MTS}$-IRES2-eGFP, *Apaf-1*$^{-/-}$ MEFs became highly sensitive to STS (51.3%) (Fig. 6A, right panels).

Smac/Diablo can induce apoptosis by IAP-dependent and IAP-independent pathways (35). To ensure that the increased apoptotic response observed in STS-treated *Apaf-1*$^{-/-}$ MEFs was due to sequestration of XIAP and not other proapoptotic functions of Smac, we used embelin, a cell-permeable small-molecular-weight inhibitor of XIAP (27). Previous work determined the 50%

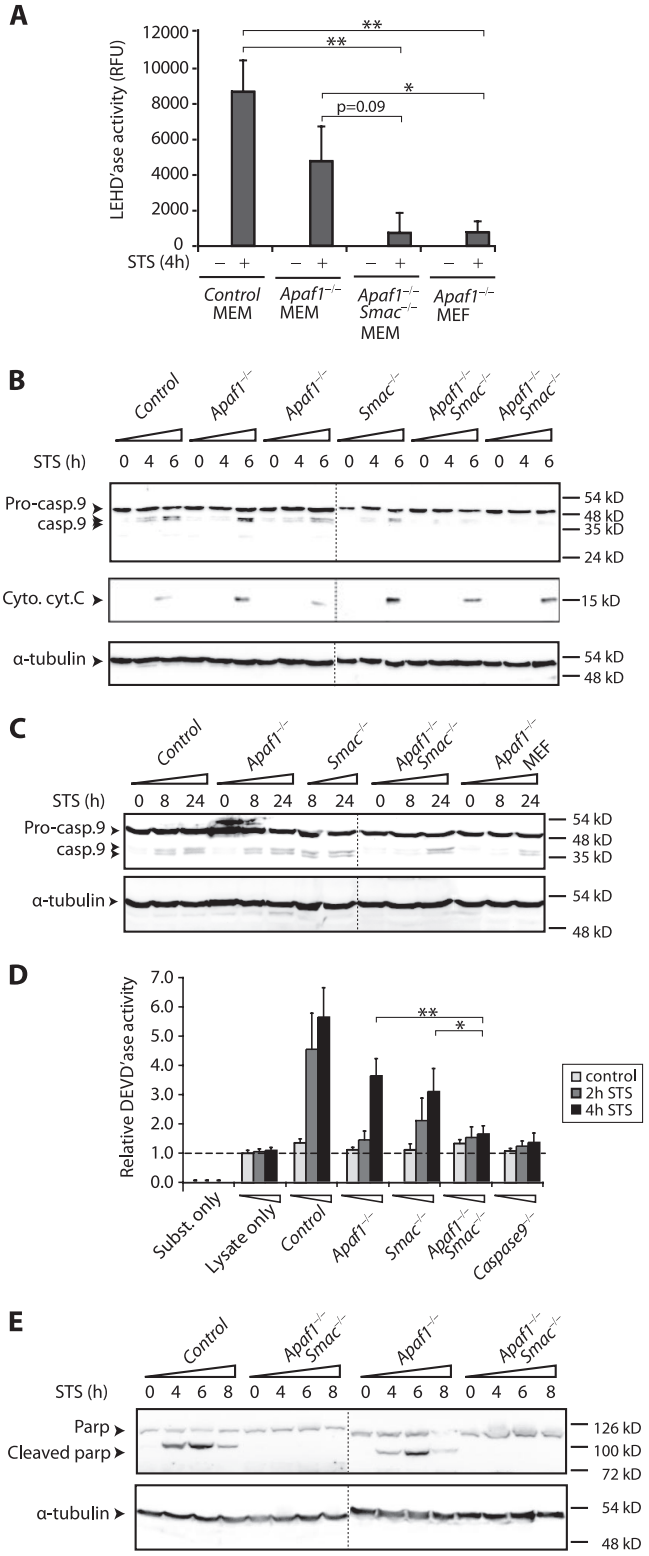

FIG. 4. Combined loss-of-function mutations in *Apaf-1* and *Smac* inhibit caspase 9 activation and processing in primary myoblasts. (A) Inhibition of caspase 9 enzymatic activity in *Apaf-1*$^{-/-}$ *Smac*$^{-/-}$ double mutant myoblasts. Cytosolic fractions from treated or untreated cultures were analyzed for caspase 9 enzymatic activity with the fluorogenic substrate LEHD 4 h post-STS treatment. The bar graphs and standard error bars were calculated from the means of three independent experiments, and the corresponding standard deviations, respectively. * and ** indicate significant differences at $P < 0.05$ and $P < 0.001$, respectively, by the Student *t* test. RFU, relative fluorescence units. (B) Inhibition of caspase 9 processing in *Apaf-1*$^{-/-}$ *Smac*$^{-/-}$ double mutant myoblasts. Cultures were exposed to 2 μM STS for the indicated periods; cytosolic fractions were collected and analyzed by Western blotting with an antibody that recognizes both the 49-kDa procaspase 9 (Pro-casp.9) and processed 39- and 37-kDa caspase 9 (Casp.9). Immunoblotting with cytochrome *c* (Cyto. cyt. C) demonstrates similar kinetics of mitochondrial release in all cultures. α-tubulin served as a loading control. The vertical dotted lines in panels B, C, and E separate two Western blots analyzed in parallel. (C) Similar delays in the kinetics of caspase 9 processing in *Apaf-1*$^{-/-}$ *Smac*$^{-/-}$ myoblasts and *Apaf-1*$^{-/-}$ fibroblasts. Caspase 9 cleavage was analyzed at the indicated time points as for panel B. (D) Inhibition of caspase 3/caspase 7 enzymatic activity, using DEVD substrate in *Apaf-1*$^{-/-}$ *Smac*$^{-/-}$ mutant myoblasts. The horizontal dotted line marks the lysate-only controls. (E) Inhibition of PARP cleavage in cytosolic fractions of *Apaf-1*$^{-/-}$ *Smac*$^{-/-}$ but not *Apaf-1*$^{-/-}$ mutant myoblasts following STS treatment.

effective dose of embelin to be 50 μM (27). We observed that at 30 μM, embelin alone did not induce caspase enzymatic activity or annexin V reactivity (Fig. 6B and C). When combined with STS, the addition of embelin to *Apaf-1*$^{-/-}$ fibroblasts increased the percentage of annexin V-positive cells by four- to sevenfold (Fig. 6D; see Fig. S2E and S3 in the supplemental material).

Induction of apoptosis in *Apaf-1*$^{-/-}$ fibroblasts by embelin was even more dramatic when combined with E2F1. In a typical experiment, infection of *Apaf-1*$^{-/-}$ MEFs with Ad.E2F1-GFP alone induced a marginal apoptotic response (~4%) (Fig. 6E). However, when combined with embelin, E2F1 induced massive apoptosis in *Apaf-1* mutant fibroblasts (~80%).

The induction of apoptosis in *Apaf-1*$^{-/-}$ MEFs by embelin plus STS was accompanied by Apaf1-independent stimulation of caspase activity, as measured in vitro with the synthetic substrate LEHD-AMC (Fig. 6F). Importantly, treatment with STS and embelin also induced the processing of procaspase 9 in the absence of Apaf-1 (Fig. 6G). Thus, in fibroblasts, caspase 9 activation and the onset of cell death can occur in the absence of Apaf-1 as long as XIAP is sequestered (by Smac/Diablo) or inhibited (by embelin).

We next asked whether the resistance to apoptosis observed in *Apaf-1*$^{-/-}$ *Smac*$^{-/-}$ double mutant myoblasts (Fig. 2B to D) was due to an increase in XIAP activity and was therefore reversible by embelin. To this end, we measured the level of annexin V-positive *Apaf-1*$^{-/-}$ *Smac*$^{-/-}$ double mutant myoblasts treated with vehicle, STS, or STS plus embelin for 3 h. As expected, STS treatment alone did not increase the level of annexin V-positive *Apaf-1*$^{-/-}$ *Smac*$^{-/-}$ myoblasts (3.76%) (Fig. 2E). However, combined treatment of these cells with STS plus embelin induced over a fivefold increase in apoptotic response (20%). The resensitization of *Apaf-1*$^{-/-}$ *Smac*$^{-/-}$ myoblasts to STS by embelin indicates that the resistance of these cells to STS treatment alone is due to the accumulation of XIAP.

MOMP is required for Apaf-1-independent caspase 9 activation in the absence of XIAP. Caspase 9 activation and apoptotic responses were induced by XIAP inhibitors only in the presence of apoptotic stimuli (STS or E2F1), suggesting that MOMP and the subsequent release of a mitochondrial factor other than cytochrome *c* or Smac/Diablo may be required for Apaf-1-independent caspase activation. To further investigate this idea, we

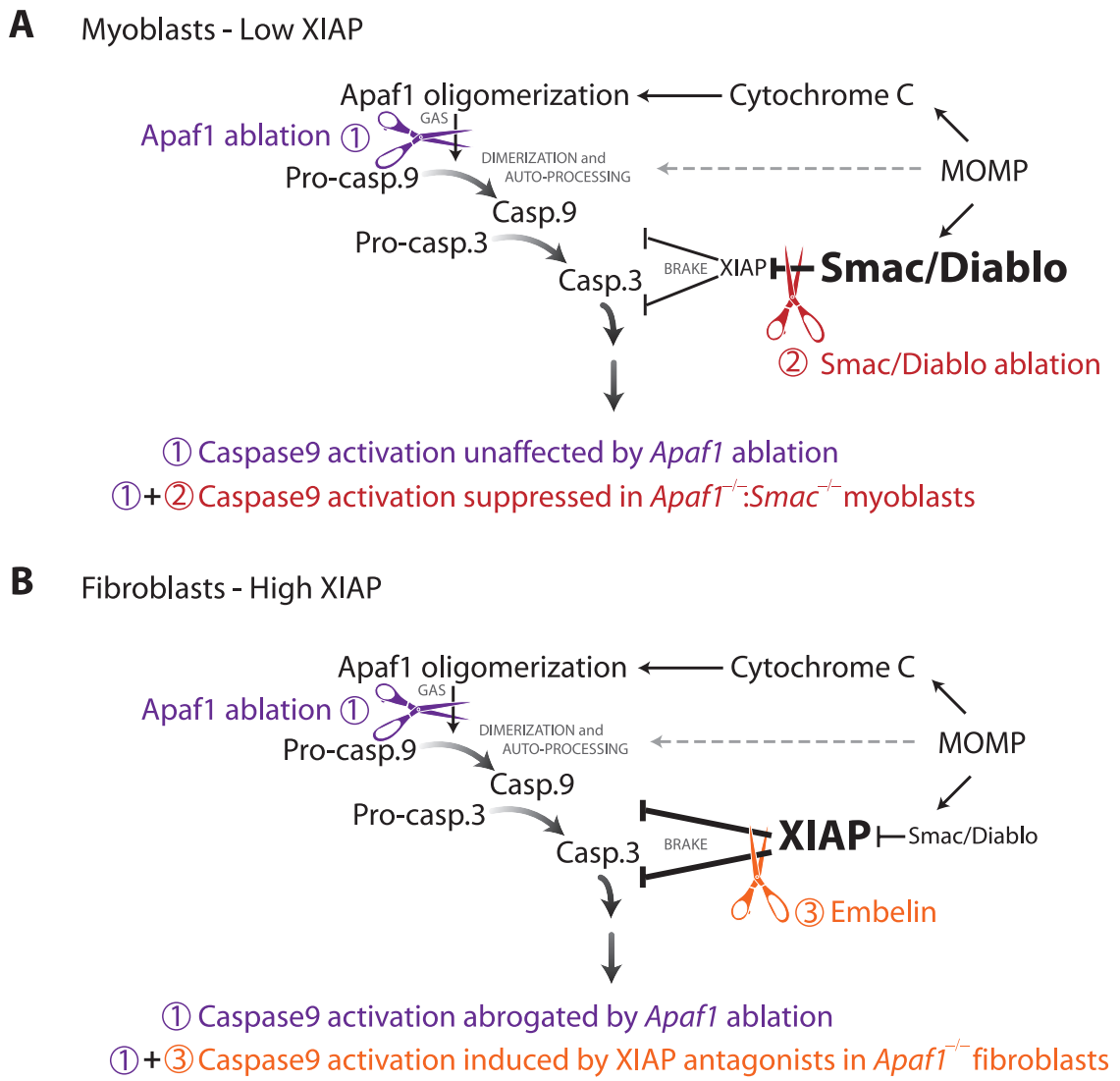

FIG. 5. Models for the proposed effects of XIAP on Apaf-1-dependent and -independent caspase 9 activation. Upon MOMP, cytochrome *c* and Smac/Diablo, as well as procaspase 9 or a novel factor yet to be defined, are released from the mitochondria (see text for details). Casp., caspase.

tested whether the cell death induced in *Apaf-1*$^{-/-}$ MEFs by embelin plus STS could be suppressed by cyclosporine (CsA), a MOMP inhibitor (34). As we showed previously (15), CsA suppressed apoptosis induced by STS in wild-type MEFs and *Apaf-1*$^{-/-}$ MEMs by about 40 to 50% (Fig. S3). Importantly, CsA also suppressed apoptosis induced by treatment with STS plus embelin in *Apaf-1*$^{-/-}$ MEFs by 48% (Fig. S3). We conclude that, while inhibition of XIAP is required for Apaf-1-independent processing of procaspase 9, it is not sufficient; MOMP and possibly the release of an additional mitochondrial factor, yet to be identified, are also required.

DISCUSSION

Caspase 9 activation can be uncoupled from Apaf-1 in skeletal myoblasts but not fibroblasts (15) (Fig. 1A). Using *Apaf-1*$^{-/-}$ *Smac*$^{-/-}$ compound mutant mice and pharmacological drugs, we showed that in primary *Apaf-1*$^{-/-}$ myoblasts, caspase 9 activation is independent of Apaf-1, due to efficient inhibition of XIAP and/or related proteins by Smac/Diablo, which accumulates in the cytosols of these cells upon drug treatment. We also showed that combined inactivation of Apaf-1 and Smac/Diablo inhibits caspase 9 activation in primary myoblasts. Thus, our results demonstrate that both the cytochrome *c*-Apaf-1 and Smac-XIAP pathways must be disrupted in order to prevent the activation of caspase 9 in response to apoptotic stimuli (Fig. 2 to 5). Indeed, in experiments done in parallel, *Apaf-1*$^{-/-}$ *Smac*$^{-/-}$ myoblasts exhibited a level of resistance to apoptotic signals similar to that of *caspase 9*$^{-/-}$ myoblasts (Fig. 2B and 4D) and *Apaf-1*$^{-/-}$ fibroblasts (Fig. 2C and 4A and C). The observation that embelin induces an apoptotic response in STS-treated *Apaf-1*$^{-/-}$ *Smac*$^{-/-}$ myoblasts (Fig. 2E) also implicates XIAP in resistance to apoptosis in these cells.

Annexin V positivity, caspase 9 processing and activation, and PARP cleavage are all slightly delayed (~1 h) in *Apaf-1*$^{-/-}$ myoblasts compared with those in wild-type myoblasts (Fig. 4).

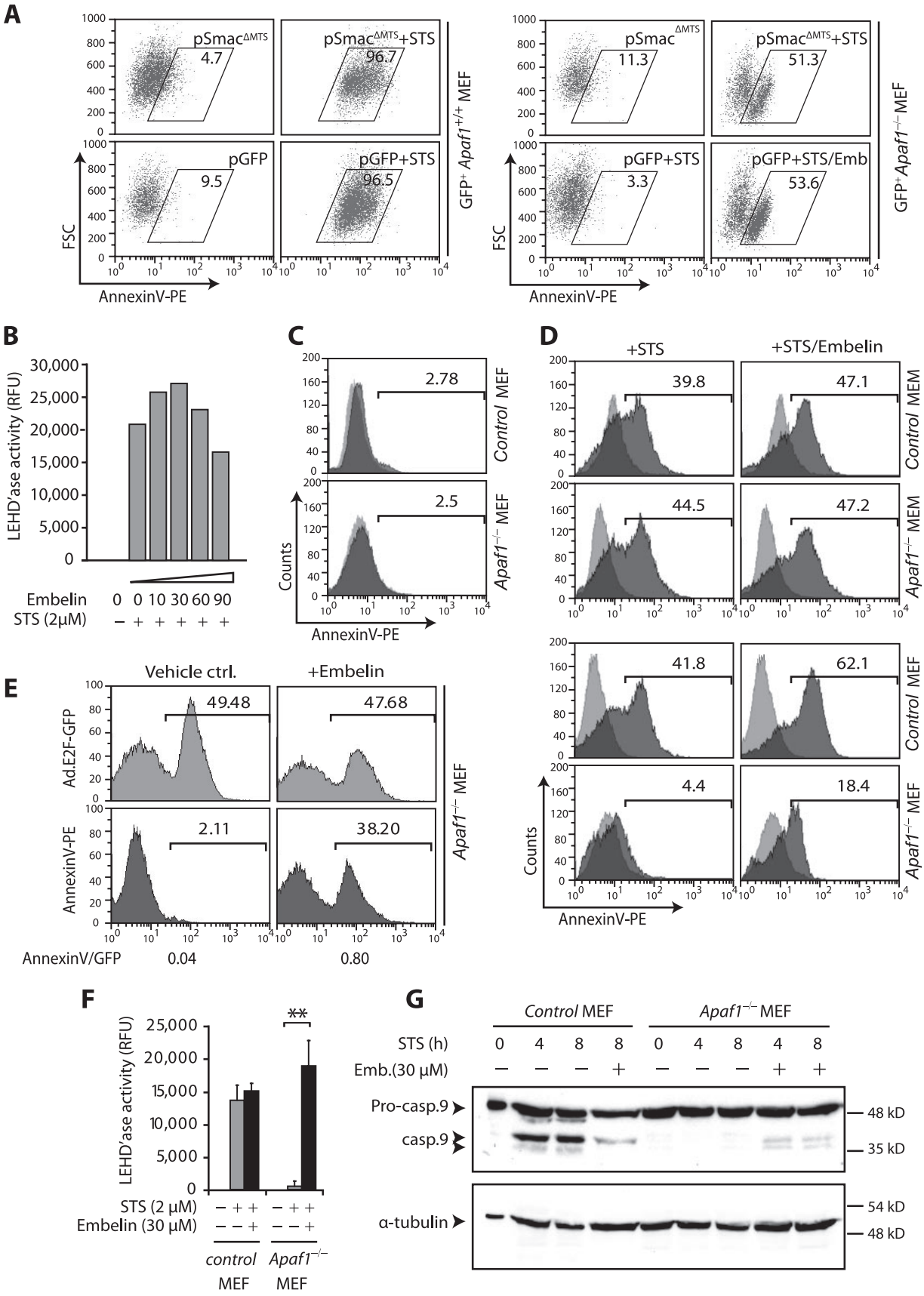
A
pSmac^ΔMTS
4.7
pSmac^ΔMTS+STS
96.7
pGFP
9.5
pGFP+STS
96.5
GFP+ Apaf1+/+ MEF
FSC
AnnexinV-PE
pSmac^ΔMTS
11.3
pSmac^ΔMTS+STS
51.3
pGFP+STS
3.3
pGFP+STS/Emb
53.6
GFP+ Apaf1−/− MEF
B
LEHD'ase activity (RFU)
Embelin 0 0 10 30 60 90
STS (2μM) − + + + + +
C
2.78
2.5
Control MEF
Apaf1−/− MEF
Counts
AnnexinV-PE
D
+STS
+STS/Embelin
39.8
47.1
44.5
47.2
41.8
62.1
4.4
18.4
Control MEM
Apaf1−/− MEM
Control MEF
Apaf1−/− MEF
Counts
AnnexinV-PE
E
Vehicle ctrl.
+Embelin
49.48
47.68
2.11
38.20
Ad.E2F-GFP
AnnexinV-PE
Apaf1−/− MEF
AnnexinV/GFP 0.04 0.80
F
LEHD'ase activity (RFU)
**
STS (2 μM) − + + − + +
Embelin (30 μM) − − + − − +
control MEF
Apaf1−/− MEF
G
Control MEF
Apaf1−/− MEF
STS (h) 0 4 8 8 0 4 8 4 8
Emb.(30 μM) − − − + − − − + +
Pro-casp.9
casp.9
α-tubulin
48 kD
35 kD
54 kD
48 kD

We suggest that this delay reflects the absence of the apoptosome and the amount of time required for Smac/Diablo to accumulate in the cytosol, sequester the low levels of XIAP expressed in myoblasts, and allow caspase 9 autoactivation. In contrast, in wild-type myoblasts, where both the cytochrome *c*-Apaf-1 and Smac/Diablo-IAP pathways are intact, efficient caspase 9 activation via the apoptosome occurs shortly after the release of cytochrome *c* and Smac/Diablo. These results are consistent with the notion that either Apaf-1 induction or XIAP inhibition can independently promote caspase 9 activation.

It was previously shown that *Apaf-1*$^{-/-}$ cells undergo cell death after prolonged exposure to cytotoxic drugs, possibly by caspase-independent apoptosis via AIF (2, 4, 5, 9, 45). We found that caspase 9 is processed 24 h posttreatment in both *Apaf-1*$^{-/-}$ *Smac*$^{-/-}$ myoblasts and *Apaf-1*$^{-/-}$ fibroblasts (Fig. 4C). This delayed, *Apaf-1*-independent caspase 9 activation may also contribute to the incomplete resistance of these mutant cells to apoptotic stimuli in long-term assays.

In fibroblasts, Apaf-1 is thought to be absolutely required for caspase 9 activation and caspase 9-mediated apoptosis (13, 50). However, we showed that fibroblasts express high levels of XIAP relative to Smac/Diablo and that inhibition of the former by overexpression of Smac/Diablo or a pharmacological antagonist induces efficient caspase 9 activation and apoptotic response even in *Apaf-1*$^{-/-}$ fibroblasts (Fig. 6). Thus, our results suggest that Apaf-1 may not be absolutely required for caspase 9 activation in vivo, as is commonly thought. Instead, the Apaf-1 requirement for caspase 9 activation and caspase 9-mediated apoptosis are cell type specific and reflect the relative levels of cytosolic Smac/Diablo and XIAP.

Loss of Smac alone does not compromise survival; *Smac*$^{-/-}$ mutant mice are alive and sensitive to various apoptotic insults (28). HtrA2/Omi, a serine protease released from mitochondria upon MOMP was thought to have IAP binding functions similar to those of Smac. However, *HtrA2/Omi*$^{-/-}$ mice do not show evidence of reduced cell death, and this phenotype is not altered in *HtrA2/Omi*$^{-/-}$ *Smac*$^{-/-}$ compound mutant mice (26). When placed on an *Apaf-1*-null background, our results finally revealed a biological role for Smac/Diablo in controlling XIAP inhibition of caspases, at least in myoblasts.

Is XIAP alone responsible for the Apaf-1-independent apoptosis observed here or are other IAPs involved? Caspase 9 activation and apoptosis were induced in *Apaf-1*$^{-/-}$ MEFs not only by Smac, which binds all IAPs, but also by embelin, a specific inhibitor of XIAP (Fig. 2E and 6). While these observations indicate that the induction of apoptosis is due to XIAP rather than caspase-independent proapoptotic functions of Smac, they do not rule out the possibility that other IAPs, in addition to XIAP, may be involved. We note that there is growing evidence that XIAP is the only IAP that inhibits caspases. The other IAPs, including cIAP-1 and cIAP-2, do not harbor several motifs (in the peptide strands surrounding BIR2 and BIR3) found in XIAP which are required for caspase inhibition and are believed to promote survival by other mechanisms (7, 8). One approach to discern between these possibilities is to knock down XIAP by small interfering/short hairpinRNA technology. However, so far we are unable to infect primary myoblasts with lentivirus-short hairpinRNA-GFP and sort and analyze the GFP-positive cells without inducing senescence. Another possible direction is to generate myoblasts from *Apaf-1*$^{-/-}$ *XIAP*$^{-/-}$ double mutant mice(14). However, while acute inactivation of XIAP may promote apoptosis, chronic inactivation of the protein in *XIAP*$^{-/-}$ mice may induce compensatory pathways that may mask XIAP function.

Our findings appear to differ from results for *Drosophila*, where the Apaf-1 homolog, Dark, is required for apoptosis induced by mutations in *Diap1*, the fly IAP homolog (36). The fly data promoted the view that caspase activation requires both "stepping on the gas" (activating Apaf-1) and "releasing the brakes" (removing XIAP) (Fig. 5) (37). In contrast, our results with mammalian myoblasts and fibroblasts demonstrate that caspase activation and apoptosis can be mediated by either mechanism, that inhibition of Apaf-1 alone does not block caspase 9 activation, and that suppression of both pathways is required to inhibit caspase 9 activation and the onset of apoptosis. The discrepancy between the fly data and our results may be due to differences in efficacy of dimerization, autoprocessing, or distinct subcellular localization of procaspase 9 in mammals versus *Drosophila* or the presence of additional mitochondrial apoptogenic factors in mammalian cells that can facilitate caspase 9 activation in the absence of Apaf-1 (see below). Other discernible differences in caspase activation among vertebrates, flies, and nematodes have been documented (20), suggesting that the mechanisms of caspase activation via the intrinsic pathway may be diverse and species specific. Notably, however, recent studies indicated that even in *Drosophila*, deletion of *Dark* abrogates cell death induced by DIAP1 inhibi-

FIG. 6. XIAP antagonists induce caspase 9 activation and apoptosis in *Apaf-1*$^{-/-}$ MEFs. (A) pSmac$^{\Delta MTS}$-IRES2-eGFP (pSmac) induces apoptosis in STS-treated *Apaf-1*$^{-/-}$ MEFs. The indicated cultures were first transfected with pSmac or empty vector (pGFP) and were then treated with STS alone or STS plus embelin for 4 h. GFP-positive cells were gated and presented as forward scatter (FSC) versus annexin V-PE. (B) Primary MEFs were treated with 2 μM STS and the indicated concentrations of embelin for 4 h; caspase 9 enzymatic activity was assessed using the fluorogenic substrate LEHD. RFU, relative fluorescence units. (C) The indicated MEFs were treated with vehicle or 30 μM embelin for 4 h and then assessed by an annexin V binding assay. (D) Embelin induces apoptosis in STS-treated *Apaf-1*$^{-/-}$ MEFs. The indicated MEF and MEM cultures were treated for 4 h with vehicle (dimethyl sulfoxide) alone, 2 μM STS, or 2 μM STS plus 30 μM embelin (STS/Emb). Apoptotic response was assessed by an annexin V assay. (E) Embelin cooperates with E2F1 to induce apoptosis in *Apaf-1*$^{-/-}$ MEFs. *Apaf-1*$^{-/-}$ MEFs were infected with Ad.E2F1-IRES-eGFP. The cultures were treated with vehicle alone or vehicle plus embelin (30 μM) and stained 24 h later with annexin V-PE. Relative apoptosis (annexin V-positive cells) normalized for infection efficiency (GFP-positive cells) is indicated by the AnnexinV/GFP ratio. ctrl., control. (F) Embelin induces caspase 9 enzymatic activity in STS-treated *Apaf-1*$^{-/-}$ MEFs. Wild-type or *Apaf-1*$^{-/-}$ MEFs were treated with vehicle alone, STS, or STS plus embelin for 4 h. Bar graph and standard error bars represent the corrected means of six independent experiments and the corresponding standard deviations. (G) Embelin induces caspase 9 processing in STS-treated *Apaf-1*$^{-/-}$ MEFs. Wild-type or *Apaf-1*$^{-/-}$ MEFs were treated with vehicle alone, STS, or STS plus embelin for the indicated intervals and then analyzed by Western blotting with caspase 9-specific antibodies. Emb., embelin; casp., caspase.

tion in most, but not all, cell types, suggesting that even in this organism caspases may be activated via the intrinsic pathway in the absence of *Dark* (1, 44).

Caspase 9 is thought to dimerize only at high concentrations created by the apoptosome in vivo or during purification and crystallization in vitro; it is otherwise predominantly monomeric (33). Our data indicate that Apaf-1 is not essential for caspase 9 activation in drug-treated cells as long as XIAP is inhibited. In agreement with our findings, a recent report shows that the level of Apaf-1 is reduced in postmitotic cardiomyocytes and that the Smac/Diablo-XIAP axis plays a central role in regulating apoptosis in these cells (31). Our results demonstrate plasticity in the two pathways even in cells (myoblasts and fibroblasts) that normally rely on both. The requirement for Apaf-1 has recently been shown to be strain dependent; on a pure C57BL/6 background, *Apaf-1*$^{-/-}$ mice are recovered at a near Mendelian ratio (29). Given our results, it would be interesting to test the cytosolic XIAP-to-Smac ratio in 129/sv versus C57BL/6 mice.

Smac or embelin induced caspase 9 activation only in the presence of MOMP inducers. In addition, using a MOMP inhibitor, CsA, we showed that MOMP is required for the apoptotic response observed in *Apaf-1* mutant fibroblasts treated with STS plus embelin (see Fig. S3 in the supplemental material). Thus, inhibition of XIAP is necessary but not sufficient to induce processing of caspase 9 in the absence of Apaf-1. Procaspase 9 was reported to reside in the mitochondria in normal cells, including skeletal muscles, and to be released into the cytosol only upon MOMP (21, 46). Thus, MOMP may be required to release procaspase 9 into the cytosol, and provided XIAP is antagonized, this may be sufficient for caspase 9 autodimerization, autoactivation, and apoptosis, even in the absence of Apaf-1. We have tested this possibility but detected caspase 9 in both cytosolic and mitochondria fractions in untreated primary MEFs and MEMs (A. T. Ho and E. Zacksenhaus, unpublished data). Nonetheless, MOMP may be required to release the mitochondrial fraction of procaspase 9 and increase its cytosolic concentration beyond a critical threshold level, thereby allowing efficient aggregation and autoprocessing in the absence of XIAP. Future studies may unravel whether caspase 9 alone, another known factor (17), or a novel factor is released upon MOMP to facilitate the Apaf-1-independent caspase 9 activation observed herein. Regardless of the mechanism, our findings demonstrate that caspase 9 activation and the onset of apoptosis can be induced in mammalian cells independently of Apaf-1 by modulating XIAP activity.

Cancer cells often escape apoptosis by elevating the levels of antiapoptotic Bcl-2 proteins or by reducing the levels of Bax, thereby inhibiting MOMP. Yet in other normal and malignant cells, factors directly downstream of MOMP clearly affect apoptosis. For example, mutations in *Apaf-1* or *caspase 9* in the mouse reduce cell death, leading to neuronal outgrowth (13, 28, 50). In Apaf-1-positive tumors, overexpression of XIAP often increases resistance to chemotherapy; inhibition of XIAP in combination with cytotoxic drugs accelerates cell death in such tumor cells (38, 39). Reduced Apaf-1 levels observed in subsets of melanoma, acute myelogenous leukemia, acute lymphoblastic leukemia, glioblastoma, and other malignancies was shown to lead to resistance to cytotoxic insults (41, 42). In light of our results, it will be important to determine whether such Apaf-1-deficient tumor cells can be induced to undergo apoptosis by combinatorial drug treatment with cytotoxic drugs plus IAP inhibitors.

ACKNOWLEDGMENTS

We thank D. W. Andrews and A. D. Schimmer for discussions and Y. Ben-David and S. E. Egan for critical comments on the manuscript.

A.T.H was supported by a fellowship from the Heart and Stroke Foundation of Canada. This work was supported by a grant to E.Z. from the Canadian Institute for Health Research (number 68809).

REFERENCES

1. **Akdemir, F., R. Farkas, P. Chen, G. Juhasz, L. Medveď ova, M. Sass, L. Wang, X. Wang, S. Chittaranjan, S. M. Gorski, A. Rodriguez, and J. M. Abrams.** 2006. Autophagy occurs upstream or parallel to the apoptosome during histolytic cell death. Development **133:**1457–1465.
2. **Baliga, B., and S. Kumar.** 2003. Apaf-1/cytochrome c apoptosome: an essential initiator of caspase activation or just a sideshow? Cell Death Differ. **10:**16–18.
3. **Boatright, K. M., M. Renatus, F. L. Scott, S. Sperandio, H. Shin, I. M. Pedersen, J. E. Ricci, W. A. Edris, D. P. Sutherlin, D. R. Green, and G. S. Salvesen.** 2003. A unified model for apical caspase activation. Mol. Cell **11:**529–541.
4. **Chipuk, J. E., L. Bouchier-Hayes, and D. R. Green.** 2006. Mitochondrial outer membrane permeabilization during apoptosis: the innocent bystander scenario. Cell Death Differ. **13:**1396–1402.
5. **Cregan, S. P., A. Fortin, J. G. MacLaurin, S. M. Callaghan, F. Cecconi, S. W. Yu, T. M. Dawson, V. L. Dawson, D. S. Park, G. Kroemer, and R. S. Slack.** 2002. Apoptosis-inducing factor is involved in the regulation of caspase-independent neuronal cell death. J. Cell Biol. **158:**507–517.
6. **Du, C., M. Fang, Y. Li, L. Li, and X. Wang.** 2000. Smac, a mitochondrial protein that promotes cytochrome c-dependent caspase activation by eliminating IAP inhibition. Cell **102:**33–42.
7. **Eckelman, B. P., and G. S. Salvesen.** 2006. The human anti-apoptotic proteins cIAP1 and cIAP2 bind but do not inhibit caspases. J. Biol. Chem. **281:**3254–3260.
8. **Eckelman, B. P., G. S. Salvesen, and F. L. Scott.** 2006. Human inhibitor of apoptosis proteins: why XIAP is the black sheep of the family. EMBO Rep. **7:**988–994.
9. **Ekert, P. G., S. H. Read, J. Silke, V. S. Marsden, H. Kaufmann, C. J. Hawkins, R. Gerl, S. Kumar, and D. L. Vaux.** 2004. Apaf-1 and caspase-9 accelerate apoptosis, but do not determine whether factor-deprived or drug-treated cells die. J. Cell Biol. **165:**835–842.
10. **Galluzzi, L., N. Larochette, N. Zamzami, and G. Kroemer.** 2006. Mitochondria as therapeutic targets for cancer chemotherapy. Oncogene **25:**4812–4830.
11. **Green, D. R.** 2005. Apoptotic pathways: ten minutes to dead. Cell **121:**671–674.
12. **Guo, Z., Y. Shi, Y. Hiroki, T. W. Mak, and E. Zacksenhaus.** 2001. Inactivation of the retinoblastoma tumor suppressor induces Apaf-1 dependent and independent apoptotic pathways during embryogenesis. Cancer Res. **61:**8395–8400.
13. **Hakem, R., A. Hakem, G. S. Duncan, J. T. Henderson, M. Woo, M. S. Soengas, A. Elia, J. L. de la Pompa, D. Kagi, W. Khoo, J. Potter, R. Yoshida, S. A. Kaufman, S. W. Lowe, J. M. Penninger, and T. W. Mak.** 1998. Differential requirement for caspase 9 in apoptotic pathways in vivo. Cell **94:**339–352.
14. **Harlin, H., S. B. Reffey, C. S. Duckett, T. Lindsten, and C. B. Thompson.** 2001. Characterization of XIAP-deficient mice. Mol. Cell. Biol. **21:**3604–3608.
15. **Ho, A., H. Li, R. Hakem, T. W. Mak, and E. Zacksenhaus.** 2004. Coupling of caspase-9 to Apaf-1 in response to loss of pRb or cytotoxic drugs is cell type dependent. EMBO J. **23:**460–472.
16. **Ho, A. T., and E. Zacksenhaus.** 2004. Splitting the apoptosome. Cell Cycle **3:**446–448.
17. **Jiang, X., H. E. Kim, H. Shu, Y. Zhao, H. Zhang, J. Kofron, J. Donnelly, D. Burns, S. C. Ng, S. Rosenberg, and X. Wang.** 2003. Distinctive roles of PHAP proteins and prothymosin-alpha in a death regulatory pathway. Science **299:**223–226.
18. **Jiang, X., and X. Wang.** 2000. Cytochrome c promotes caspase-9 activation by inducing nucleotide binding to Apaf-1. J. Biol. Chem. **275:**31199–31203.
19. **Jiang, X., and X. Wang.** 2004. Cytochrome *c*-mediated apoptosis. Annu. Rev. Biochem. **73:**87–106.
20. **Kornbluth, S., and K. White.** 2005. Apoptosis in Drosophila: neither fish nor fowl (nor man, nor worm). J. Cell Sci. **118:**1779–1787.
21. **Krajewski, S., M. Krajewska, L. M. Ellerby, K. Welsh, Z. Xie, Q. L. Deveraux, G. S. Salvesen, D. E. Bredesen, R. E. Rosenthal, G. Fiskum, and J. C. Reed.** 1999. Release of caspase-9 from mitochondria during neuronal apoptosis and cerebral ischemia. Proc. Natl. Acad. Sci. USA **96:**5752–5757.

22. **Lakhani, S. A., A. Masud, K. Kuida, G. A. Porter, Jr., C. J. Booth, W. Z. Mehal, I. Inayat, and R. A. Flavell.** 2006. Caspases 3 and 7: key mediators of mitochondrial events of apoptosis. Science **311:**847–851.
23. **Li, P., D. Nijhawan, I. Budihardjo, S. M. Srinivasula, M. Ahmad, E. S. Alnemri, and X. Wang.** 1997. Cytochrome c and dATP-dependent formation of Apaf-1/caspase-9 complex initiates an apoptotic protease cascade. Cell **91:**479–489.
24. **Liu, X., C. N. Kim, J. Yang, R. Jemmerson, and X. Wang.** 1996. Induction of apoptotic program in cell-free extracts: requirement for dATP and cytochrome c. Cell **86:**147–157.
25. **Marsden, V. S., L. O'Connor, L. A. O'Reilly, J. Silke, D. Metcalf, P. G. Ekert, D. C. Huang, F. Cecconi, K. Kuida, K. J. Tomaselli, S. Roy, D. W. Nicholson, D. L. Vaux, P. Bouillet, J. M. Adams, and A. Strasser.** 2002. Apoptosis initiated by Bcl-2-regulated caspase activation independently of the cytochrome c/Apaf-1/caspase-9 apoptosome. Nature **419:**634–637.
26. **Martins, L. M., A. Morrison, K. Klupsch, V. Fedele, N. Moisoi, P. Teismann, A. Abuin, E. Grau, M. Geppert, G. P. Livi, C. L. Creasy, A. Martin, I. Hargreaves, S. J. Heales, H. Okada, S. Brandner, J. B. Schulz, T. Mak, and J. Downward.** 2004. Neuroprotective role of the Reaper-related serine protease HtrA2/Omi revealed by targeted deletion in mice. Mol. Cell. Biol. **24:**9848–9862.
27. **Nikolovska-Coleska, Z., L. Xu, Z. Hu, Y. Tomita, P. Li, P. P. Roller, R. Wang, X. Fang, R. Guo, M. Zhang, M. E. Lippman, D. Yang, and S. Wang.** 2004. Discovery of embelin as a cell-permeable, small-molecular weight inhibitor of XIAP through structure-based computational screening of a traditional herbal medicine three-dimensional structure database. J. Med. Chem. **47:**2430–2440.
28. **Okada, H., W. K. Suh, J. Jin, M. Woo, C. Du, A. Elia, G. S. Duncan, A. Wakeham, A. Itie, S. W. Lowe, X. Wang, and T. W. Mak.** 2002. Generation and characterization of Smac/DIABLO-deficient mice. Mol. Cell. Biol. **22:** 3509–3517.
29. **Okamoto, H., H. Shiraishi, and H. Yoshida.** 2006. Histological analyses of normally grown, fertile Apaf1-deficient mice. Cell Death Differ. **13:**668–671.
30. **Pop, C., J. Timmer, S. Sperandio, and G. S. Salvesen.** 2006. The apoptosome activates caspase-9 by dimerization. Mol. Cell **22:**269–275.
31. **Potts, M. B., A. E. Vaughn, H. McDonough, C. Patterson, and M. Deshmukh.** 2005. Reduced Apaf-1 levels in cardiomyocytes engage strict regulation of apoptosis by endogenous XIAP. J. Cell Biol. **171:**925–930.
32. **Reed, J. C.** 2006. Proapoptotic multidomain Bcl-2/Bax-family proteins: mechanisms, physiological roles, and therapeutic opportunities. Cell Death Differ. **13:**1378–1386.
33. **Renatus, M., H. R. Stennicke, F. L. Scott, R. C. Liddington, and G. S. Salvesen.** 2001. Dimer formation drives the activation of the cell death protease caspase 9. Proc. Natl. Acad. Sci. USA **98:**14250–14255.
34. **Ricci, J. E., N. Waterhouse, and D. R. Green.** 2003. Mitochondrial functions during cell death, a complex (I-V) dilemma. Cell Death Differ. **10:**488–492.
35. **Roberts, D. L., W. Merrison, M. MacFarlane, and G. M. Cohen.** 2001. The inhibitor of apoptosis protein-binding domain of Smac is not essential for its proapoptotic activity. J. Cell Biol. **153:**221–228.
36. **Rodriguez, A., P. Chen, H. Oliver, and J. M. Abrams.** 2002. Unrestrained caspase-dependent cell death caused by loss of Diap1 function requires the Drosophila Apaf-1 homolog, Dark. EMBO J. **21:**2189–2197.
37. **Salvesen, G. S., and J. M. Abrams.** 2004. Caspase activation—stepping on the gas or releasing the brakes? Lessons from humans and flies. Oncogene **23:**2774–2784.
38. **Schimmer, A. D., S. Dalili, R. A. Batey, and S. J. Riedl.** 2006. Targeting XIAP for the treatment of malignancy. Cell Death Differ. **13:**179–188.
39. **Schimmer, A. D., K. Welsh, C. Pinilla, Z. Wang, M. Krajewska, M. J. Bonneau, I. M. Pedersen, S. Kitada, F. L. Scott, B. Bailly-Maitre, G. Glinsky, D. Scudiero, E. Sausville, G. Salvesen, A. Nefzi, J. M. Ostresh, R. A. Houghten, and J. C. Reed.** 2004. Small-molecule antagonists of apoptosis suppressor XIAP exhibit broad antitumor activity. Cancer Cell **5:**25–35.
40. **Shiozaki, E. N., J. Chai, D. J. Rigotti, S. J. Riedl, P. Li, S. M. Srinivasula, E. S. Alnemri, R. Fairman, and Y. Shi.** 2003. Mechanism of XIAP-mediated inhibition of caspase-9. Mol. Cell **11:**519–527.
41. **Soengas, M. S., P. Capodieci, D. Polsky, J. Mora, M. Esteller, X. Opitz-Araya, R. McCombie, J. G. Herman, W. L. Gerald, Y. A. Lazebnik, C. Cordon-Cardo, and S. W. Lowe.** 2001. Inactivation of the apoptosis effector Apaf-1 in malignant melanoma. Nature **409:**207–211.
42. **Soengas, M. S., W. L. Gerald, C. Cordon-Cardo, Y. Lazebnik, and S. W. Lowe.** 2006. Apaf-1 expression in malignant melanoma. Cell Death Differ. **13:**352–353.
43. **Spierings, D., G. McStay, M. Saleh, C. Bender, J. Chipuk, U. Maurer, and D. R. Green.** 2005. Connected to death: the (unexpurgated) mitochondrial pathway of apoptosis. Science **310:**66–67.
44. **Srivastava, M., H. Scherr, M. Lackey, D. Xu, Z. Chen, J. Lu, and A. Bergmann.** 2007. ARK, the Apaf-1 related killer in Drosophila, requires diverse domains for its apoptotic activity. Cell Death Differ. **14:**92–102.
45. **Susin, S. A., E. Daugas, L. Ravagnan, K. Samejima, N. Zamzami, M. Loeffler, P. Costantini, K. F. Ferri, T. Irinopoulou, M. C. Prevost, G. Brothers, T. W. Mak, J. Penninger, W. C. Earnshaw, and G. Kroemer.** 2000. Two distinct pathways leading to nuclear apoptosis. J. Exp. Med. **192:**571–580.
46. **Susin, S. A., H. K. Lorenzo, N. Zamzami, I. Marzo, C. Brenner, N. Larochette, M. C. Prevost, P. M. Alzari, and G. Kroemer.** 1999. Mitochondrial release of caspase-2 and -9 during the apoptotic process. J. Exp. Med. **189:**381–394.
47. **Vaux, D. L., and J. Silke.** 2005. IAPs, RINGs and ubiquitylation. Nat. Rev. Mol. Cell. Biol. **6:**287–297.
48. **Verhagen, A. M., P. G. Ekert, M. Pakusch, J. Silke, L. M. Connolly, G. E. Reid, R. L. Moritz, R. J. Simpson, and D. L. Vaux.** 2000. Identification of DIABLO, a mammalian protein that promotes apoptosis by binding to and antagonizing IAP proteins. Cell **102:**43–53.
49. **Wei, M. C., W. X. Zong, E. H. Cheng, T. Lindsten, V. Panoutsakopoulou, A. J. Ross, K. A. Roth, G. R. MacGregor, C. B. Thompson, and S. J. Korsmeyer.** 2001. Proapoptotic BAX and BAK: a requisite gateway to mitochondrial dysfunction and death. Science **292:**727–730.
50. **Yoshida, H., Y. Y. Kong, R. Yoshida, A. J. Elia, A. Hakem, R. Hakem, J. M. Penninger, and T. W. Mak.** 1998. Apaf1 is required for mitochondrial pathways of apoptosis and brain development. Cell **94:**739–750.
51. **Zacksenhaus, E., Z. Jiang, D. Chung, J. Marth, R. A. Phillips, and B. L. Gallie.** 1996. pRb controls cell proliferation, differentiation and death of skeletal muscle cells and other lineages during embryogenesis. Genes Dev. **10:**3051–3064.
52. **Zou, H., Y. Li, X. Liu, and X. Wang.** 1999. An APAF-1.cytochrome *c* multimeric complex is a functional apoptosome that activates procaspase-9. J. Biol. Chem. **274:**11549–11556.